Molecularly imprinted N-doped TiO_2 photocatalysts for the selective degradation of o-phenylphenol fungicide from water

Roberto Fiorenza[*a,b], *Alessandro Di Mauro*[a], *Maria Cantarella*[a] *Antonino Gulino*[b], *Luca Spitaleri*[b], *Vittorio Privitera*[a], *and Giuliana Impellizzeri*[a]

[a] *CNR-IMM, Via S. Sofia 64, 95123 Catania, (Italy).*

[b] *Department of Chemistry, University of Catania, Viale Andrea Doria 6, 95125 Catania, (Italy).*

*** Corresponding author**

E-mail address: rfiorenza@unict.it

Abstract

In this work it is investigated the photodegradation of a widely used fungicide, i.e. the orto-phenylphenol (o-p.p.), through molecularly imprinted N-doped TiO_2 photocatalysts. The materials have been prepared by the sol-gel technique with an easy one-pot synthesis method. The structural, textural, and surface properties of the samples were evaluated by scanning electron microscopy (SEM), N_2 adsorption-desorption measurements, X-ray photoelectron (XPS) and UV-vis diffuse reflectance spectroscopies (DRS), whereas the Fourier transform infrared spectroscopy (FTIR) was performed to check the effectiveness of the molecular imprinting process. The synergistic mechanism between the molecular imprinting (that allow to obtain a selective photodegradation), N-doping (which permits to boost the photoactivity under solar light irradiation), and the photocatalysis leads to obtain selective and efficient photocatalysts for wastewater purification.

Keywords: Photocatalysis, TiO_2, Wastewater Treatment, Fungicide, Molecular Imprinting, Nitrogen.

1. Introduction

Nowadays, one of the most important problem of the modern society is the scarcity of water and its pollution. The extensive use of agricultural products, as fertilizer and pesticides, and the large amount of water required for the agricultural practises make this industrial activity one of the most crucial for the quality of the aquatic ecosystems. In the last years, the advanced oxidation process (AOP), and in particular the photocatalysis, has emerged as a performing green solution for the removal of recalcitrant pollutants in water [1-4]. The photocatalytic process consists on the generation of non-selective highly-reactive radicals (such as, the hydroxyl radicals) which are able to completely oxidise the organic contaminants [5, 6].

The lack of selectivity it is one of the drawbacks of the photocatalysis. Indeed, in a typical water polluted effluent only the contaminants present at high concentration are efficiently degraded (usually the less-toxic compounds), whereas the contaminants present at low concentration (usually the highly-toxic substances), such as the pesticides, are poorly degraded. The photocatalyst synthesis driven by the molecular imprinting technique is an attractive approach to obtain selective materials [7-10]. It involves the formation of reversible/week interactions between the photocatalyst and the target contaminant during the first steps of the material synthesis, followed by the removal of the template (i.e., the target pollutant) by elution methods or thermal treatments. In this way, through the modification of the pores and cavities of the catalyst, it is possible to obtain a selective interaction between the photocatalytic material and the pollutant. The changed pores and cavities are, indeed, the recognition sites for the target contaminant and, subsequently, thorough the photocatalytic process a selective photodegradation can be obtained. In our recent papers, we successfully applied this combined approach (i.e., molecular imprinting + photocatalysis) to wastewater purification. In particular,

molecularly imprinted ZnO and TiO_2 were employed for selective photodegradation of pharmaceuticals and pesticides under UV light irradiation [11-13].

In this work, we extended the photocatalytic performance of TiO_2 in the visible range rendering the material more attractive from a practical point of view [14-16]. As largely reported in the literature, the doping of TiO_2 with nitrogen promotes the photoactivity under solar or visible light irradiation [17-19]. We synthetized molecularly imprinted N-doped TiO_2 materials with a simple sol-gel route. The as-prepared samples were tested under simulated solar light irradiation, for the photodegradation of a widely used fungicide, i.e. the o-phenylphenol which its residue in water or in the soil can induce problems in growth, in fertility, and in kidneys [20]. The proposed approach is, therefore, a combination of three methodologies: molecular imprinting, doping process, and photocatalytic oxidation, with the conclusive aim of obtaining a selective and solar light active TiO_2 photocatalysts.

On the basis of the above considerations, the substantial novelties of the present work are:

a) The easy, simple and green materials synthesis: it allows to obtain, with a one-pot procedure, molecularly imprinted photocatalytic materials activated by the solar/visible light irradiation. The absence of an organic/polymer matrix and the contemporary use of a nitrogen salt precursor is a process not yet explored in the literature.

b) In our previous works [12,13] the combined approach: molecular imprinting + photocatalysis was analysed for the degradation of different pesticides (2,4D herbicide and imidacloprid insecticide) under UV light irradiation. Instead, in this manuscript, we have also investigated the doping process, to shift the activity of the TiO_2-based photocatalysts towards the solar/visible light irradiation (more appealing considering a possible scale-up application). Furthermore, another kind of pesticide, i.e. the o-

phenylphenol fungicide has been used as target contaminant and as template for the molecular imprinting process. On the best of our knowledge, only one work [21] investigates the use of this template for the molecular imprinting, nevertheless in this cited work the authors have studied molecularly imprinted polymer (MIP) materials for the extraction of o-phenylphenol from blood serum and river water.

Thus, the exploration of the visible light photocatalytic performance of inorganic (i.e. without polymer matrix) molecularly imprinted materials is an issue poorly examined in the literature. Finally, however the mineralization efficiency of the examined catalysts was not high, due to the recalcitrant nature of the analysed pesticide, the achieved selectivity under solar irradiation is a promising result as starting point for the development of selective/solar-activated materials to overcome one of the drawbacks of the photocatalysis, as the lack of selectivity. The obtaining of selective photocatalysts, is indeed, an important aim in the field of the current wastewater treatments for the efficient removal of the emergent water contaminants as the pesticides. These hazardous compounds, in fact, are usually present in the water effluents at low concentrations and they are not degraded by the conventional photo-activated materials that preferentially oxidizing the less-toxic pollutants present in the water at high concentrations. With the molecular imprinting it is possible, as investigated in this work, obtaining selective photocatalysts for the removal of pesticides from water.

2. Experimental

2.1. Catalyst preparation

The molecularly imprinted N-doped TiO_2 samples were synthesized using the sol-gel technique. The stoichiometry amount of o-phenylphenol ($C_{12}H_{10}O$, shorten in o-p.p.) required to obtain a molar ratio of 5:1 between TiO_2 and the fungicide was dissolved in a

solution of 0.5 ml of acetic acid and 1.5 ml of ethanol; then the solution was stirred at room temperature until a complete solubilization of the pesticide. Successively, 2 ml of titanium butoxide was added in the mixture and it was stirred for further 10 min. Then, a solution containing 2 ml of demineralized water, 2 ml of ethanol and the appropriate amount of ammonium nitrate (NH_4NO_3) as nitrogen precursors, was added dropwise to the above solution. The resultant slurry was stirred for 3 hrs, and aged for 24 hrs. The obtained wet gel was dried at 100 °C for 12 hrs, and then calcined in air at 500 °C for 6 hrs. The samples were labelled as "Nx%-MI TiO_2/o-p.p.", where "x" indicates the atomic percentage of nitrogen. The un-doped samples, called "MI TiO_2/o-p.p." were prepared with the same procedure described above but without the use of NH_4NO_3, i.e. the nitrogen precursor. The bare TiO_2, simply named "TiO_2" was synthesized without the addition of both the ammonium nitrate and the pesticide.

2.2. Catalyst characterization

The morphology of the materials was investigated by scanning electron microscopy (SEM), with a field emission Zeiss Supra 25 microscope. The textural properties of the samples were measured by the adsorption-desorption of N_2 at -196 °C, after a pre-treatment of out-gassing at 100 °C overnight, using a Micromeritics Tristar II 3020 equipment. Fourier transform infrared spectroscopy (FTIR) spectra were acquired through a Perkin-Elmer Spectrum 1000 spectrometer. X-ray photoelectron spectroscopy (XPS) analyses were carried out at 45° take-off angle relative to the surface plane, with a PHI 5600 Multi Technique system. Samples were excited with Al Kα X-ray radiation using a pass energy of 5.85 eV. Structures due to the Kα satellite radiations were subtracted from the spectra prior to data processing. The XPS peak intensities were obtained after Shirley background removal; the instrumental energy resolution was ≤ 0.5 eV and the spectra calibration was achieved by fixing the main C 1s signal at 285.0 eV

[22]. UV-vis diffuse reflectance (DRS) spectra were obtained by using a Perkin-Elmer Lambda 40 UV-vis spectrophotometer.

2.3. Photocatalytic activity experiments

The selective photodegradation of o-p.p. was investigated under solar irradiation using a ORIEL LSS-7120 Solar Simulator system (400-1100 nm, irradiance: 1 kW/m^2). Before any measurements the samples were irradiated by a UV lamp for 90 min in order to eliminate the hydrocarbons from their surface [23]. A quantity of 1 mg of catalyst powders was added to 4 ml of aqueous solution of o-p.p. (1×10^{-4} M) in quartz cuvettes. The solutions were treated by ultrasonic irradiations (50 Hz for 5 min) to favour the dispersion of the powders. Control experiments were performed in the dark for 90 min to reach the adsorption-desorption equilibrium. Every 30 min (for a final time of 4 hrs), the irradiated solutions were measured with an UV-vis spectrophotometer (Lambda 45, Perkin-Elmer), in a wavelength range of 200-700 nm. Before any measurements, the materials were centrifuged for 3 min with a spin of 1500 rpm, to remove the powders and consequently reduce the light scattering phenomena. The degradation of o-p.p. was estimated by the absorbance peaks at 282 nm in the Lambert-Beer regime.

The selectivity of the photocatalysts was verified evaluating the degradation of phenol (1×10^{-4} M, compound with a similar chemical structure of o-p.p.) following in this case the absorbance peak at 270 nm. Furthermore, it was carried out a photodegradation test with a mixture solution of o-p.p. and phenol (2 ml o-p.p. 1×10^{-4} M + 2 ml phenol 1×10^{-4} M) following the same experimental conditions reported above.

The extent of the mineralization after the photocatalytic tests was determined measuring the total organic carbon (TOC) content with a TOC analyzer (Shimadzu TOC-LCSH) equipped with a non-dispersive infrared detector (NDIR). The inorganic carbon was removed from the analysed solutions by adding HCl and successively purging with

dry air, then the TOC content was evaluated after a high-temperature catalytic oxidation at 680°C.

3. Results and discussion

Figure 1 reports the SEM images of "TiO_2", "MI TiO_2/o-p.p." and "N1.6%-MI TiO_2/o-p.p.", as representative samples. An irregular morphology with heterogeneous shaped particles, typical of the matrix-free sol-gel synthesis [24] characterized all the investigated samples, irrespective of the molecular imprinting or the doping processes. The textural properties of the investigated samples, obtained by Brunauer-Emmett-Teller (BET) adsorption-desorption of N_2, are reported in Table 1. The "MI TiO_2/o-p.p" sample showed a decrease of BET surface area compared to the TiO_2 (95 m^2/g respect to 100 m^2/g of bare TiO_2) with a consequent increase of about 1 nm in the mean pore diameter (6 nm instead of 5 nm of un-imprinted TiO_2). It is interesting to note that this increase of the mean pore diameter is strictly in line with the molecular length of the o-p.p. (0.9 nm, estimated by Chem-Draw© program). The addition of the nitrogen precursor had as effect a moderate enhancement in the surface area (up to 118 m^2/g) and in the pore volume (Tab.1), whereas the mean pore diameters (most influenced by the molecular imprinting) remain substantially the same in all the N-doped samples (around 6 nm). The insertion and the subsequent removal of the o-p.p. during the preparation of the molecularly imprinted TiO_2 varied the porosity of the titanium dioxide with the formation of larger pores and cavities, which will be the recognition sites for the selective photodegration of the fungicide.

Table 1 also reports the band-gap energies, E_g, of the semiconductors, as estimated by UV-vis DRS spectra using the Kubelka–Munk method [25]. The data revealed that the addition of nitrogen did not substantially altered the band-gap energy of TiO_2, which remains in the range of 3.2-3.0 ± 0.3 eV.

The XPS characterization is summarized in Tab. 2. Bare TiO_2 and "MI TiO_2/o-p.p." samples showed the Ti $2p_{3/2, 1/2}$ spin-orbit components in the range 459.9-459.8 eV and 465.6-465.5 eV, respectively, together with the O 1s band at 531.1-531.0 eV, consistently with the reported values for the TiO_2 in the anatase phase [26]. These peaks present in all the investigated samples clearly evidenced the crystalline phase of anatase, as expected for a calcination process at 500 °C. An important evidence is the absence of low binding energy broadening of the TiO_2 doublet. This fact suggests the substantial absence of Ti ions in a 3^+ valence state. Indeed, the eventual existence of these ions should be detected with a XPS spectrum containing a pair of overlapping Ti 2p doublets, due to the contribution of various final state screening effects [27]. The band of N 1s is located for all the N-doped investigated samples at 400.2-400.4 eV. These values are ascribed to the interstitial nitrogen whereas peaks at low binding energies (397 eV), absent in the investigated materials, characterize the substitutional nitrogen [17,18,28]. The formation of interstitial nitrogen was further confirmed, in accordance with the literature [17,18,28], by the chemical shift at lower binding energies of the Ti $2p_{3/2, 1/2}$ and O 1s of the molecularly imprinted N-doped TiO_2 anatase powders (Tab. 2). The measured surface amount of nitrogen was rather similar to the nominal one (Tab. 2), confirming the doping process of the molecularly imprinted TiO_2 with interstitial nitrogen.

The occurrence of the molecular imprinting process was verified by the FTIR measurements and reported in Fig. 2. The FTIR spectra of the o-p.p. exhibited nine peculiar bands: those at 1591, 1485 and 1450 cm^{-1} are related to the C=C vibrations of the aromatic ring [29], the O−H bending is identified with the band at 1360 cm^{-1}, the C−O stretching is detected at 1240 cm^{-1}, whereas the bands at 1173 and 1065 cm^{-1} are the signals of the CH aromatic vibration and the C−OH vibration, respectively [30]. Lastly, the bands at 830 and 760 cm^{-1} are characteristic of the CH aromatic out of plane [29,30].

Interestingly, the sample not calcined (coded as "MI TiO_2/o-p.p. Not removed") displayed some fingerprint bands of the fungicide, and in particular some bands are shifted compared to the o-phenylphenol. These data clearly confirmed the formation of an interaction between the Ti-O-Ti backbone and the pesticide. After the calcination process the FTIR spectrum of the "MI TiO_2/o-p.p." sample is similar to that of bare TiO_2, pointing to the complete removal of the fungicide thanks to the thermal treatment, and the successfully synthesis of the molecularly imprinted TiO_2 catalyst. With the addition of the ammonium nitrate (i.e., the nitrogen precursor) it is also possible to note the presence of some bands of the o-p.p. before the calcination (we report as representative sample the "N0.4%-MI TiO_2/o-p.p. Not removed") together with a band at 1425 cm^{-1} related to the asymmetric stretching mode of NO_3^- [31]. As expected, after the annealing at 500 °C the removal of the pesticide and the incorporation of nitrogen on the crystalline structure of TiO_2 occurred; indeed, the spectra of the N-doped samples are analogous to the bare TiO_2, with a band at 1626 cm^{-1} assigned to the bending vibration of the O−H group of residual water molecules, and a wider band in the range of 700-500 cm^{-1} due to the Ti−O−Ti stretching vibration modes [30].

Figure 3A illustrates the photodegradation of o-p.p. fungicide under simulated solar light irradiation thanks to the analysed samples. The experimental error of the photocatalytic test was 1% (i.e., within the symbol size). No substantial contribution of the adsorption process was detected during 90 min in the dark, in accordance with the literature and our previous papers [7, 11-13]. The absence of a preferential adsorption of the pesticide on the imprinted materials can be explained through the formation of week and reversible interactions between the pesticide/target and the imprinted TiO_2 dissolved in the solution [12, 13]. When the solar light was switched on, no relevant degradation was measured in the experiment without any photocatalysts (o-p.p. curve in Fig. 3A), as

expected. A slight increase in the degradation efficiency with the un-modified TiO_2 (7%) and "MI TiO_2/o-p.p." catalyst (12%) is evidenced. The observed TiO_2 activity under solar light is probably due to wavelengths in the UVA region of the used solar simulator. The "MI TiO_2/o-p.p." samples showed a higher photocatalytic efficiency with respect to bare TiO_2, because of the modified pores/cavities, shaped through the molecular imprinting process with the same pesticide/target. A further increase of the o-p.p. photodegradation efficiency was obtained thanks to the N-doped molecularly imprinted samples. The increasing can be explained by the combination of the shape-selectivity, gained through the molecular imprinting process, and the nitrogen doping, which makes the materials sensitive to the visible light. The kinetic constant (calculated considering a pseudo-first order kinetic [32;33]) of "N0.4%-MI TiO_2/o-p.p." ($(15\pm2)\times10^{-4}$ min^{-1}) is ~ 5 times and 3 times higher compared to the bare TiO_2 ($(3.0\pm0.3)\times10^{-4}$ min^{-1}) and "MI TiO_2/o-p.p." ($(5.0\pm0.5)\times10^{-4}$ min^{-1}). The photodegradation efficacy increases with the amount of nitrogen (up to 1.2%). In particular, the "N1.2%-MI TiO_2/o-p.p" samples degrades ~ 46% of o-p.p. with a kinetic constant of $(26\pm3)\times10^{-4}$ min^{-1}. An additional enhancement of the nitrogen amount (at 1.6%) has a detrimental effect on the photocatalytic performance, being the kinetic constant of the "N1.6%-MI TiO_2/o-p.p." catalyst $(23\pm2)\times10^{-4}$ min^{-1} similar to the one of "N1.2%-MI TiO_2/o-p.p." catalyst (i.e., $(26\pm3)\times10^{-4}$ min^{-1}). This catalytic trend was also confirmed by testing two other N-doped samples with higher nitrogen content: 2% and 4%, (data not shown). The kinetic constants of these two materials ($(11\pm1)\times10^{-4}$ min^{-1} and $(10\pm1)\times10^{-4}$ min^{-1} for "N2%-MI TiO_2/o-p.p" and "N4%-MI TiO_2/o-p.p", respectively) resulted much lower than the kinetic constant of the "N1.2%-MI TiO_2/o-p.p." that resulted the best photocatalyst for the o-p.p. removal. The occurrence of an optimal amount of nitrogen, positive for the photoactivity, is in accordance with previous works related to not imprinted N-doped TiO_2 materials

[17,19,34]. The beneficial effects of the nitrogen doping can be attributed to the location of the N species at the interstitial sites of the TiO_2 crystallographic structure, as confirmed by XPS; thus, the N atoms can act as impurity sensitizers, also influencing the TiO_2 surface defects concentration [35]. However, an excessive nitrogen doping induces a decrease of photoactivity because the surface defects present at higher concentration could also behave as recombination centres for the photo-generated electrons and holes [34]. The advantageous effects of the inclusion of nitrogen on the TiO_2 (that also favours a moderate increase of the surface area (Tab.1), beneficial for the photoactivity) lead to obtain performing solar active materials.

The photocatalytic degradation of o-phenylphenol under solar/visible light irradiation follows different degradation steps with a partial mineralization [32,33]. The most common intermediates products reported in the literature are ethyl phenethyl ether, phenyl acetaldehyde [32], hydroquinone and p-benzoquinone [33]. For this reason, even with the best performing sample (i.e. the "N1.2%-MI TiO_2/o-p.p") the removed organic carbon, evaluated by TOC analysis, was ~ 5%.

The peculiar selectivity given by the molecular imprinting was verified by photocatalytic tests using a similar compound to o-p.p.: the phenol. The results are reported in Fig. 3B. All the investigated samples showed a similar catalytic behaviour, with only a slightly higher degradation efficiency of N-doped samples. In particular, "N1.2%-MI TiO_2/o-p.p." exhibited an efficiency of ~17%, higher than the ~ 4% of "MI TiO_2/o-p.p." and of un-imprinted TiO_2 (~4%). This increase in the photoactivity can be reasonably related to the positive features of the nitrogen doping, which effects are, however, less performing for the phenol photodegradation. The lower photocatalytic performance of the molecularly imprinted catalysts towards the phenol degradation compared to the o-p.p. removal can be linked to the shape selectivity of the samples

molecularly imprinted with o-p.p. Indeed, only with the materials imprinted with the same pesticide/target to be degraded (in our case the o-p.p.) it is possible to increase significantly the photocatalytic degradation of the chosen pesticide. The "MI TiO_2/o-p.p." and the N-doped "MI TiO_2/o-p.p." catalysts, having been imprinted with the o-p.p. molecules, possess pores/cavities with size and structure dissimilar respect to phenol; for this reason, the photoactivity of the imprinted samples towards the phenol oxidation is low. Similarly to the o-p.p., also for the phenol different by-products are formed during the solar/visible light photocatalytic degradation. In detail: benzoquinone, hydroquinone, resorcinol, catechol, and organic acids [36,37] with only a small amount of CO_2 and water. Indeed, with the "N1.2%-MI TiO_2/o-p.p." sample only ~ 2% of TOC was mineralized in our experimental conditions.

To have a further proof of the achieved selectivity, an additional photocatalytic test was performed utilizing a mixed aqueous solution of o-p.p. and phenol. The results of this experiment are reported in Fig. 4. Following the o-p.p. degradation (Fig. 4A) it is possible to confirm the best activity of the "N1.2%-MI TiO_2/o-p.p." sample. In detail, the degradation efficiency (~45%) is equal, within the experimental errors, to the efficiency evaluated in pure o-phenlylphenol solution (~46%, see Fig. 3A). On the other hand, considering the phenol degradation in the mixed solution (Fig. 4B), the "N1.2%-MI TiO_2/o-p.p." sample showed only a small higher photoactivity compared to "MI TiO_2/o-p.p." and bare TiO_2 samples, as also detected in the pure phenol solution test (see Fig. 3B). These data clearly confirm the selectivity of the samples molecularly imprinted with the o-p.p.

The combination of the molecular imprinting, the N-doping and the photocatalysis leads, towards a synergistic effect, to obtain a selective and effectiveness degradation of the fungicide o-p.p. under simulated solar light irradiation. The molecular imprinting

process allows TiO_2 to selectively interact with the pesticide, the N-doping boosts the TiO_2 activity under solar light irradiation, and the photocatalytic process effectively degrades the wastewater contaminant.

4. Conclusions

The selective removal of the fungicide o-phenylphenol from wastewater was investigated by molecularly imprinted N-doped TiO_2 photocatalysts. The pesticide was utilized as templates during the sol-gel synthesis of titanium dioxide, eventually doped with nitrogen, and then it was removed through calcination. The combination between the molecular imprinting process (which allows a selective interaction between the TiO_2 and the fungicide), the nitrogen doping and the TiO_2-based photocatalysis leads to obtain a preferential photodegradation of the pesticide from water under simulated solar light irradiation. This strategy is promising to synthesize with an easy one-pot procedure, selective solar light active photocatalysts useful for water purification.

Acknowledgments

This work was partially funded by the SENTI project, ESF (European Social Found) Sicily 2020 (CUP: G67B17000160009) and has been supported by the European regional development funds (FESR) INTERREG V – A Italia Malta - Micro WatTS C1-1.1-70 (CUP: B61G18000070009).

References

[1] D.B. Miklos, C. Remy, M. Jekel, K.G. Linden, J.E. Drewes, U. Hübner, Water Research 139 (2018) 118-131.

[2] S. Kanan, M.A. Moyet, R.B. Arthur, H.H. Patterson, Catal. Rev. Sci. Eng. (2019) 1-65.

[3] M Cantarella, R Sanz, M.A. Buccheri, F Ruffino, G Rappazzo, S Scalese, G. Impellizzeri, V. Privitera, J. Photochem. Photobiol. A Chem. 321 (2016) 1-11.

[4] A Di Mauro, M Zimbone, M Scuderi, G Nicotra, M.E. Fragalà, G Impellizzeri, Nanoscale Res. Lett. 10 (1) (2015) 484.

[5] R. Fagan, D.E. McCormack, D.D. Dionysiou, S.C. Pillai, Mater. Sci. Semicond. Process 42 (2016) 2-14.

[6] A Di Mauro, M.E. Fragala, V. Privitera, G. Impellizzeri Mater. Sci. Semicond. Process 69 (2017) 44-51.

[7] D. Sharabi, Y. Paz, Appl. Catal. B Environ. 95 (2010) 169-178.

[8] Y. Wu, Y. Dong, X. Xia, X. Liu, H. Li, App. Surf. Sci. 364 (2016) 829-836.

[9] H. Shi, Y. Wang, C. Tang, W. Wang, M. Liu, G. Zhao, Appl. Catal. B Environ. 246 (2019) 50-60.

[10] X. Luo, F. Deng, L. Min, S. Luo, B. Guo, G. Zeng, C. Au, Environ. Sci. Technol. 47 (2013) 7404-7412.

[11] M. Cantarella, A. Di Mauro, A. Gulino, L. Spitaleri, G. Nicotra, V. Privitera, G. Impellizzeri, Appl. Catal. B Environ. 238 (2018) 509-517.

[12] R. Fiorenza, A. Di Mauro, M. Cantarella, V. Privitera, G. Impellizzeri, J. Photochem. Photobiol. A Chem. 380 (2019) 111872.

[13] R. Fiorenza, A. Di Mauro, M. Cantarella, C. Iaria, E.M. Scalisi, M.V. Brundo, A. Gulino, L. Spitaleri, G. Nicotra, S. Dattilo, S.C. Carroccio, V. Privitera, G. Impellizzeri, Chem. Eng. J. 379 (2020) 122309.

[14] G. Impellizzeri, V. Scuderi, L. Romano, E. Napolitani, R. Sanz, R. Carles, V. Privitera, J. Appl. Phys., 117 (2015) 105308.

[15] G. Impellizzeri, V. Scuderi, L. Romano, P.M. Sberna, E. Arcadipane, R. Sanz, M. Scuderi, G. Nicotra, M. Bayle, R. Carles, F. Simone, V. Privitera, J. Appl. Phys., 116 (2016) 173507.

[16] V. Scuderi, G. Impellizzeri, M. Zimbone, R. Sanz, A. Di Mauro, M.A. Buccheri, M. Miritello, A. Terrasi, G. Rappazzo, G. Nicotra, V. Privitera, Appl. Catal. B Environ. 183 (2016) 328-334.

[17] O. Pikuda, C. Garlisi, G. Scandura, G. Palmisano J. Catal. 346 (2017) 109-116.

[18] P. Wang, T. Zhou, R. Wang, Teik-Thye Lim, Water Research (2011) 5015-5026.

[19] R. Fiorenza, M. Bellardita, S. Scirè, L. Palmisano, Mol. Catal. 455 (2018) 108-120.

[20] K.E. Appel, Arch. Toxicol. 74 (2000) 61-71.

[21] S. Bakhtiar, S.A. Bhawani, S. R. Shafqat, Chem. Biol. Technol. Agric. 6 (2019) 15.

[22] A. Gulino, Anal. Bioanal. Chem. 405 (2013) 1479-1495.

[23] R. Wang, K. Hashimoto, A. Fujishima, M. Chikuni, E. Kojima, A. Kitamura, M. Shimohigoshi, T. Watanabe, Nature 388 (1997) 431-432.

[24] A.K.L. Sajjad, S. Shamaila, B. Tian, F. Chen, J. Zhang, Appl. Catal. B Environ. 91 (2009) 397-405.

[25] Y.I. Kim, S.J. Atherton, E.S. Bringham, T.E. Mallouk, J. Phys. Chem. 97 (1993) 11802–11810.

[26] G. Sivalingam, K. Nagaveni, M.S. Hegde, G. Madras, Appl. Catal. B: Environ. 45 (2003) 23-38.

[27] B. Bharti, S. Kumar, H.-N. Lee, R. Kumar, Sci. Rep. 6 (2016) 32355.

[28] J. Senthilnathan, L. Philip, Chem. Eng. J. 161 (2010) 83-92.

[29] D.L. Pavia, G.M. Lampman, G.S. Kriz, J.R. Vyvyan, Introduction to Spectroscopy, fourth ed., Brooks Cole Cengage Learning, USA, 2008, 46-48.

[30] A. Davydov, Molecular Spectroscopy of Oxide Catalyst Surfaces, in: N.T. Sheppard (Ed.), John Wiley & Sons Ltd, The Atrium, Southern Gate, Chichester, West Sussex PO19 8SQ, England, 2003.

[31] H.B. Wu, M.N. Chan, C. K. Chan, Aerosol Sci. Tech. 41 (2007) 581-588.

[32] R. Hu, X. Xiao, S. Tu, X. Zuo, J. Nan, Appl. Catal. B 163 (2015) 510-519.

[33] A.A. Khodja, T. Sehili, J.F. Pilichowski, P. Boule, J. Photochem. Photobio. A: Chem. 141 (2001) 231-239.

[34] W. Wang, M.O. Tadé, Z. Shao, Prog. Mater. Sci. 92 (2018) 33-63.

[35] S. Sato, R. Nakamura, S. Abe, Appl. Catal. A: Gen. 284 (2005) 131-137.

[36] I. Hazra Chowdhury, M. Roy, S. Kundu, M.K. Naskar, J. Phys. Chem. Solids 129 (2019) 329-339.

[37] O. Sacco, V. Vaiano, C. Daniela, W. Navarra, V. Venditto, Mater. Sci. Semicond. Process 80 (2018) 104-110.

Table 1 BET Surface area (S_{BET}), mean pore diameter (D_p), pore volume (V_p) and band-gap energies (E_g) of the investigated samples.

Catalysts	**S_{BET} ($m^2 g^{-1}$)**	**D_p(nm)**	**V_p ($cm^3 g^{-1}$)**	**E_g (eV)**
TiO_2	100 ± 1	5.2 ± 0.2	0.06 ± 0.02	3.2 ± 0.3
MI TiO_2/o-p.p.	95 ± 1	6.0 ± 0.2	0.13 ± 0.02	3.2 ± 0.3
N0.4%-MI TiO_2/o-p.p.	106 ± 1	6.0 ± 0.2	0.12 ± 0.02	3.2 ± 0.3
N0.8%-MI TiO_2/o-p.p.	114 ± 1	6.2 ± 0.2	0.16 ± 0.02	3.2 ± 0.3
N1.2%-MI TiO_2/o-p.p.	118 ± 1	6.2 ± 0.2	0.23 ± 0.02	3.1 ± 0.3
N1.6%-MI TiO_2/o-p.p.	114 ± 1	6.0 ± 0.2	0.20 ± 0.02	3.0 ± 0.3

Table 2 XPS Binding Energies (eV) of the investigated samples.

Sample	**Ti $2p_{3/2,1/2}$**	**O 1s**	**N 1s**
TiO_2	459.9 465.6	531.1	-
MI TiO_2/o-p.p	459.8 465.5	531.0	-
N0.4%-MI TiO_2/o-p.p.	459.2 464.6	530.6	400.3 (0.6 at%)
N0.8%-MI TiO_2/o-p.p.	459.2 464.9	530.6	400.4 (0.8 at%)
N1.2%-MI TiO_2/o-p.p.	459.0 464.9	530.4	400.3 (1.0 at%)
N1.6%-MI TiO_2/o-p.p.	459.0 464.8	530.4	400.2 (1.4 at%)

Captions to figures

Fig. 1 SEM images of (A) TiO_2, (B) MI TiO_2/o-p.p., and (C) N1.6%-MI TiO_2/o-p.p. samples.

Fig. 2 FTIR spectra of the investigated samples. The dashed lines indicate the main bands of the o-p.p. pesticide, whereas the solid line refers to the stretching of NO_3^- group.

Fig. 3 (A) Photocatalytic degradation of o-phenylphenol under simulated solar light irradiation for o.p.p. aqueous solution (closed circles), o.p.p. aqueous solutions with: TiO_2 (closed squares), MI TiO_2/o-p.p. (closed triangles), N0.4%-MI TiO_2/o-p.p. (open circles), N0.8%-MI TiO_2/o-p.p. (closed down triangles), N1.2%-MI TiO_2/o-p.p. (open squares), N1.6%-MI TiO_2/o-p.p. (open triangles). (B) Photocatalytic degradation of phenol under simulated solar light irradiation for phenol aqueous solution (closed circles), phenol aqueous solutions with: TiO_2 (closed squares), MI TiO_2/o-p.p. (closed triangles), N0.4%-MI TiO_2/o-p.p. (open circles), N0.8%-MI TiO_2/o-p.p. (closed down triangles), N1.2%-MI TiO_2/o-p.p. (open squares), N1.6%-MI TiO_2/o-p.p. (open triangles).

Fig. 4 (A) Photocatalytic degradation of o-phenylphenol in the mixed o-phenylphenol + phenol solution under simulated solar light irradiation for o.p.p. aqueous solution (closed circles), TiO_2 (closed squares), MI TiO_2/o-p.p. (closed triangles) and N1.2%-MI TiO_2/o-p.p. (open squares). (B) Photocatalytic degradation of phenol in the mixed o-phenylphenol + phenol solution under simulated solar light irradiation for phenol aqueous solution (closed circles), TiO_2 (closed squares), MI TiO_2/o-p.p. (closed triangles) and N1.2%-MI TiO_2/o-p.p. (open squares).

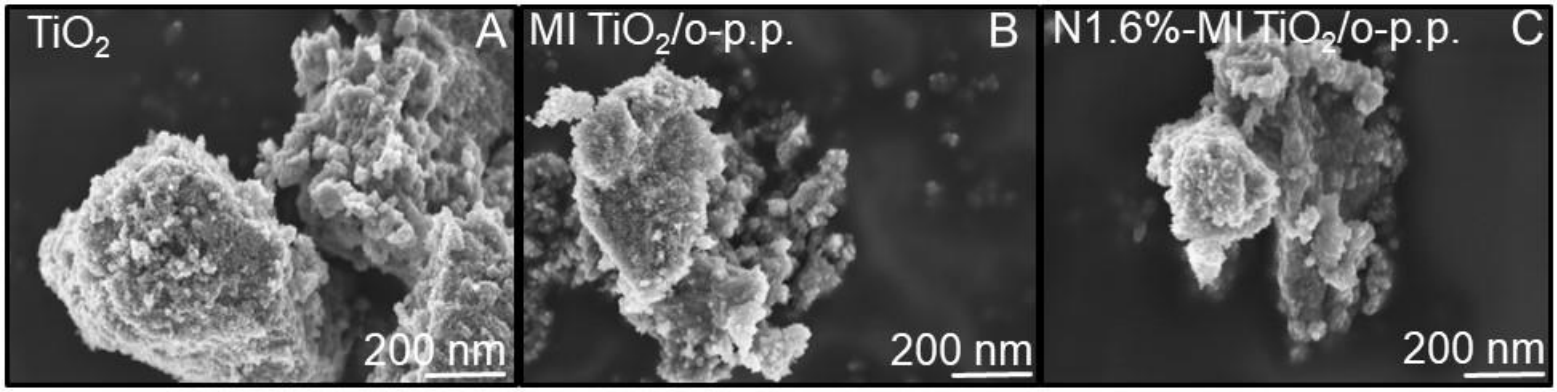

Fig. 1

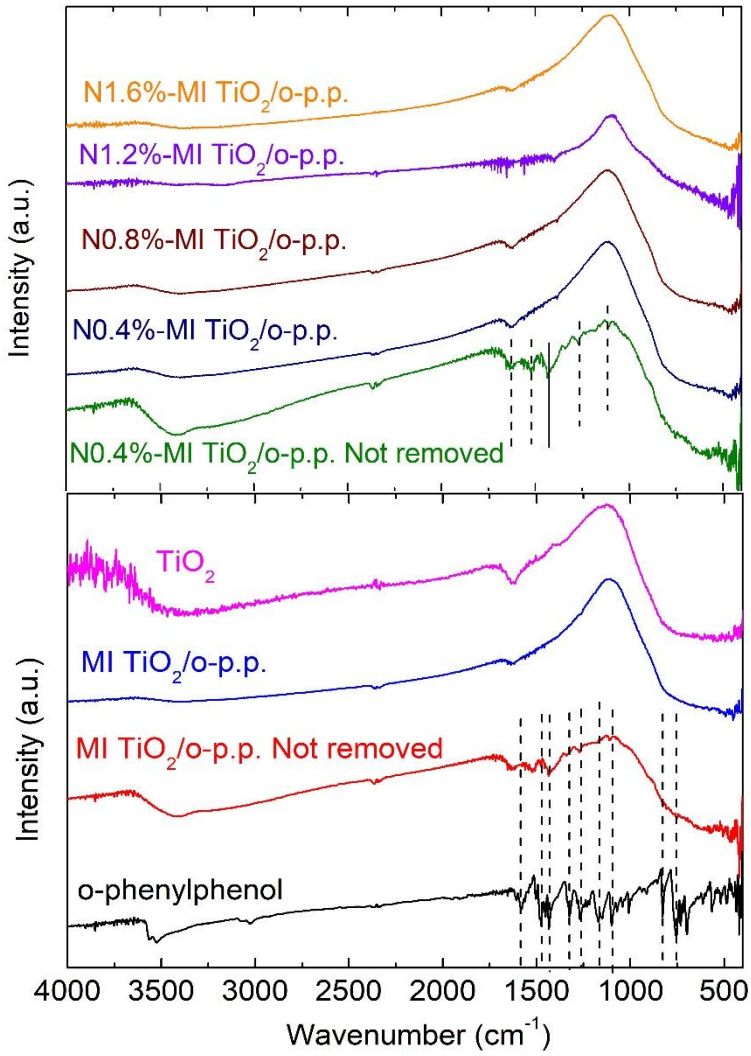
N1.6%-MI TiO2/o-p.p.
N1.2%-MI TiO2/o-p.p.
N0.8%-MI TiO2/o-p.p.
N0.4%-MI TiO2/o-p.p.
N0.4%-MI TiO2/o-p.p. Not removed
Intensity (a.u.)
TiO2
MI TiO2/o-p.p.
MI TiO2/o-p.p. Not removed
o-phenylphenol
Intensity (a.u.)
4000 3500 3000 2500 2000 1500 1000 500
Wavenumber (cm-1)

Fig. 2

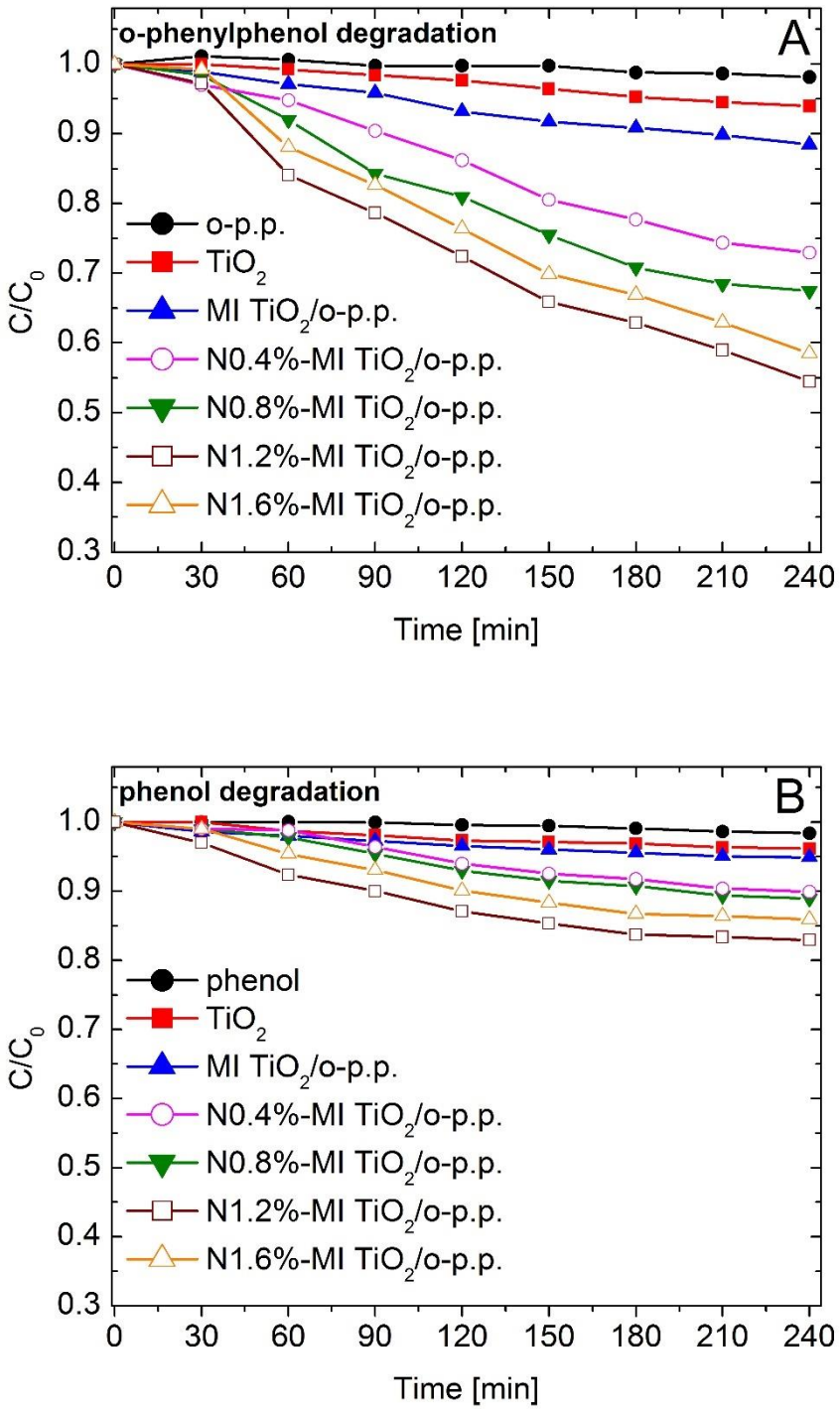
o-phenylphenol degradation
A
C/C0
Time [min]
o-p.p.
TiO2
MI TiO2/o-p.p.
N0.4%-MI TiO2/o-p.p.
N0.8%-MI TiO2/o-p.p.
N1.2%-MI TiO2/o-p.p.
N1.6%-MI TiO2/o-p.p.
phenol degradation
B
C/C0
Time [min]
phenol
TiO2
MI TiO2/o-p.p.
N0.4%-MI TiO2/o-p.p.
N0.8%-MI TiO2/o-p.p.
N1.2%-MI TiO2/o-p.p.
N1.6%-MI TiO2/o-p.p.

Fig. 3

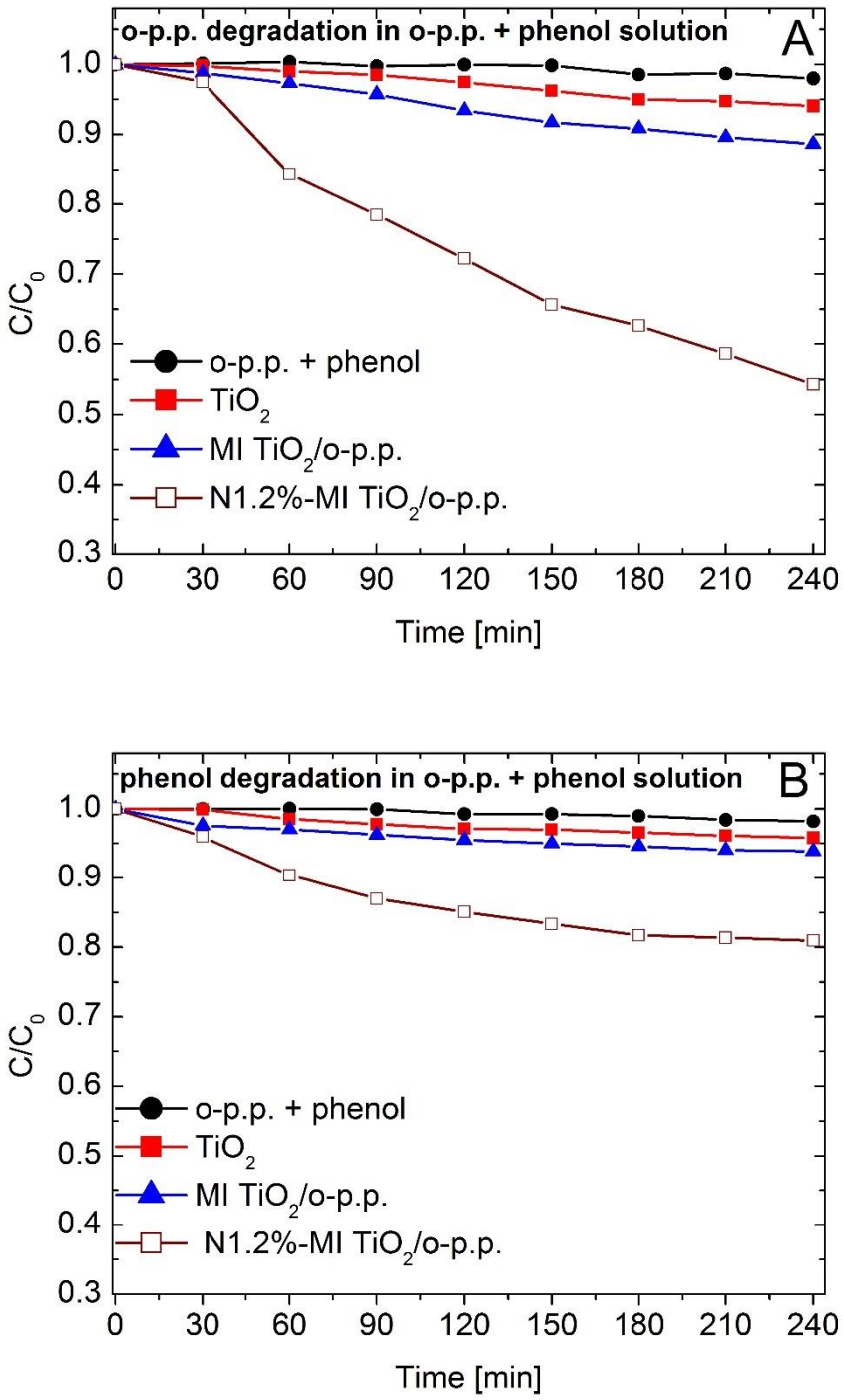
o-p.p. degradation in o-p.p. + phenol solution
A
C/C0
1.0
0.9
0.8
0.7
0.6
0.5
0.4
0.3
0
30
60
90
120
150
180
210
240
Time [min]
o-p.p. + phenol
TiO2
MI TiO2/o-p.p.
N1.2%-MI TiO2/o-p.p.
phenol degradation in o-p.p. + phenol solution
B
C/C0
Time [min]
o-p.p. + phenol
TiO2
MI TiO2/o-p.p.
N1.2%-MI TiO2/o-p.p.

Fig. 4